Available online at www.sciencedirect.com
SCIENCE DIRECT®
Journal of Nuclear Materials 325 (2004) 169–173
journal of nuclear materials
www.elsevier.com/locate/jnucmat

Electron spin resonance measurement of irradiation defects in vitreous silica irradiated with neutrons

Kimikazu Moritani, Ikuji Takagi, Hirotake Moriyama *

Department of Nuclear Engineering, Graduate School of Engineering, Kyoto University, Yoshida, Sakyo-ku, Kyoto 606-8501, Japan

Received 3 August 2003; accepted 28 November 2003

Abstract

The electron spin resonance (ESR) measurement of irradiation defects in neutron-irradiated vitreous silica was performed to study the effects of the OH content, neutron fluence, and post-irradiation isochronal anneal to 873 K. Together with the usual paramagnetic states of E′ centers, non-bridging oxygen hole centers (NBOHCs), and peroxy radicals (PORs), some new states were observed in the ESR spectra. The principal-axis g-values of these states lied in the range $g \sim 2.0$–2.2, which were typical of O_2^- ions in solids. Considering these new defects, the observed effects of the OH content, neutron fluence, and post-irradiation isochronal anneal were discussed to obtain some details of the reaction mechanism of the irradiation defects.

1. Introduction

Irradiation behavior of ceramic materials is one of the topics of current interest, since some of these materials are to be used in the strong radiation field of proposed fusion reactors. However, the production behavior of irradiation defects under neutron irradiation has not been fully clarified in spite of the considerable progress in understanding many aspects of irradiation defects in these ceramic materials. It is thus important to know the production behavior of irradiation defects in neutron irradiated ceramic materials.

In the case of vitreous silica, the three fundamental centers of the E′ center (≡Si·), the peroxy radical (POR: ≡Si—O—O·) and the non-bridging oxygen hole center (NBOHC: ≡Si—O·) are known to form the basis of the present understanding of defects in this material [1]. These are all paramagnetic and have been well characterized by the electron spin resonance (ESR) techniques, compared with the diamagnetic oxygen-deficiency centers (ODCs: ≡Si:Si≡). In addition, the self-trapped holes (STHs: ≡Si—Ȯ—Si≡) are also known to participate in the radiolysis process in the lower temperature range, and it has been recently suggested that the STHs play an important role even at the ambient temperature under irradiation [2]. Thus, it is needed to take into account all these defects in order to interpret the irradiation behavior of vitreous silica.

In the present study, the electron spin resonance (ESR) measurement of irradiation defects in neutron-irradiated vitreous silica was performed to study the effects of the OH content, neutron fluence, and post-irradiation isochronal anneal to 873 K. The obtained results are analyzed to discuss some details of the reaction mechanism of the irradiation defects.

2. Experimental

Vitreous silica (T-1030, T-2030) was obtained from Toshiba Ceramics Co., and weighed samples of 100 mg each were irradiated with thermal neutrons at a position of 2.75×10^{13} n cm^{-2} s^{-1} in the Kyoto University Research Reactor (KUR). The irradiation time ranged from 1 min to 60 min, and neutron fluence ranged from

* Corresponding author. Tel./fax: +81-75 753 5824.
E-mail address: moriyama@nucleng.kyoto-u.ac.jp (H. Moriyama).

0022-3115/$ - see front matter © 2003 Elsevier B.V. All rights reserved.
doi:10.1016/j.jnucmat.2003.11.011

Table 1
Sample and irradiation conditions

Specimen	OH (ppm)	Irradiation condition	
		Irradiation time (min)	Neutron fluence ($n\,cm^{-2}$)
T-1030	200	1–60	1.7×10^{15}–1.0×10^{17}
T-2030	1	1–60	1.7×10^{15}–1.0×10^{17}

1.7×10^{15} n cm^{-2} to 1.0×10^{17} n cm^{-2}. Table 1 summarizes the samples and irradiation conditions.

After the irradiation, first-derivative ESR spectra were recorded either at room temperature (for the E′s) or at 77 K (for others) on a JEOL JES-TE200 instrument operating at X-band frequencies ($\nu \sim 9.26$ GHz) with 100-kHz magnetic field modulation. Measurements of the g-values were accomplished by using conventional standard samples of DPPH (diphenylpicrylhydrazyl) and MgO. Ten-minute isochronal anneals in 50 K increments were carried out by moving the samples contained in fused quartz sample tubes to an external furnace. Spin concentrations were determined by resolution of derivative spectra into a number of components, double numerical integration of every component spectra and comparison of the obtained areas with that of a DPPH sample of 1.53×10^{18} spins per mg. The accuracy of the numerical integrations was typically of the order of ±5% for the stronger signals in the irradiated samples. In the case of the weaker signals, these errors were over ±10% due to low signal-to-noise ratios. As all of the ESR signals decreased in strength with increasing anneal temperature, the accuracies of the numerical integrations also decreased.

3. Results and discussion

3.1. Resolution of ESR spectra

Fig. 1 illustrates a typical ESR spectrum of neutron irradiated vitreous silica of T-1030. As shown in this figure, the resolution of the observed spectra was not completed only by considering the participation of the well-known paramagnetic defect centers of the E′, NBOHC and POR, and then some new variants of the O_2^--type defect centers were taken into account. In the resolution of each spectrum, the initial g-values and peak-to-peak derivative widths of Lorentzian line shapes for the E′, NBOHC and POR were taken from the literatures [1] and those of the O_2^--type defect centers were assumed to follow the g-value theory of Känzig and Cohen [3].

According to their theory, the g-values of O_2^- ions in solids are given by the following equations:

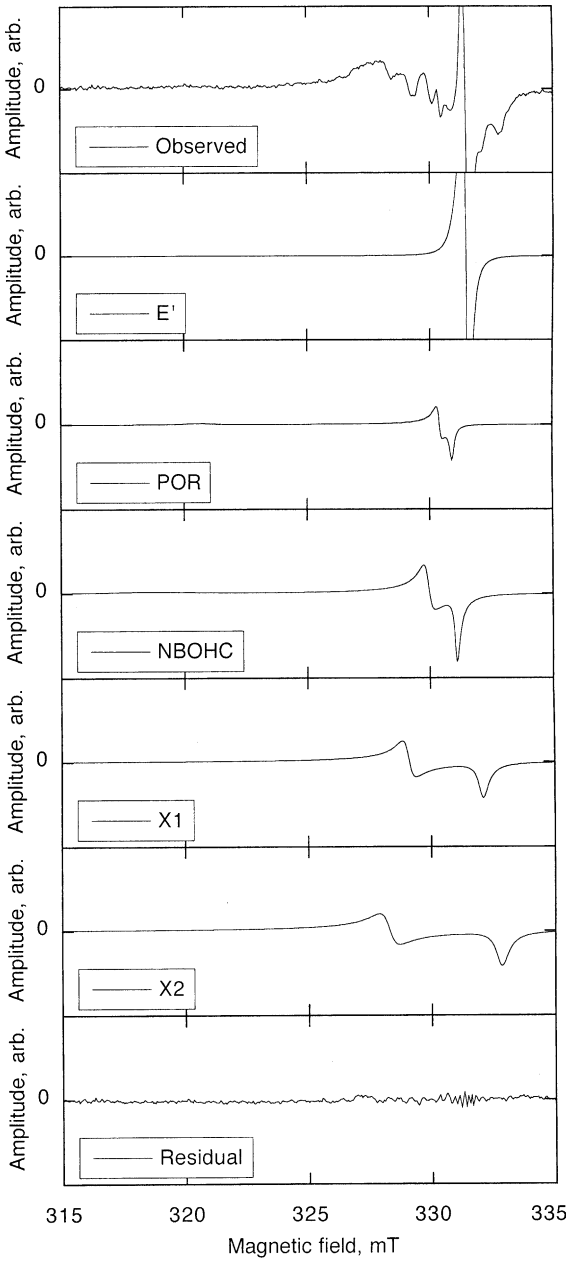

Fig. 1. Typical X-band ESR spectrum of the neutron-irradiated high OH silica (T-1030) and its components: (a) observed spectrum (1.6×10^{16} n cm^{-2}), (b) E′, (c) POR, (d) NBOHC, (e) X_1, (f) X_2, and (g) others.

$$g_1 = g_e\left(\frac{\Delta^2}{\lambda^2+\Delta^2}\right)^{1/2} - \frac{\lambda}{E}\left[-\left(\frac{\lambda^2}{\lambda^2+\Delta^2}\right)^{1/2} - \left(\frac{\Delta^2}{\lambda^2+\Delta^2}\right)^{1/2} + 1\right], \quad (1)$$

$$g_2 = g_e\left(\frac{\Delta^2}{\lambda^2+\Delta^2}\right)^{1/2} - \frac{\lambda}{E}\left[\left(\frac{\lambda^2}{\lambda^2+\Delta^2}\right)^{1/2} - \left(\frac{\Delta^2}{\lambda^2+\Delta^2}\right)^{1/2} - 1\right], \quad (2)$$

$$g_3 = g_e + 2\left(\frac{\lambda^2}{\lambda^2+\Delta^2}\right)^{1/2} l, \quad (3)$$

where g_e is the free-electron g-value (2.00232), λ the spin–orbit coupling constant for the O^- ion, Δ the splitting of the 2p π_g antibonding level, E the separation of the foregoing level from 2p σ_g bonding level ($E = 5.08$ eV for O_2^- ions in NaCl [4]), and l is a correction to the orbital angular momentum ($l = 1$ for the free molecular ion). With a constraint of these equations, a line shape simulation was performed similarly to the case of the literatures [5–7], and a least squares fitting method was applied to the simulation in order to determine the g-values and peak-to-peak derivative widths of the component defects. The results are summarized in Table 2.

The principal-axis g-values for the new variant of the O_2^--type defect centers, which are denoted by X_1 and X_2, are different from those of the well known paramagnetic states of the E′s, NBOHCs, and PORs. These are attributed to some other minor states considering their production behavior. In fact, the production yield has been observed to saturate with the increasing neutron fluence as shown below. Thus, the production of these states might be hardly observed in the case of highly irradiated samples [8].

3.2. Neutron fluence dependence of spin densities

Figs. 2 and 3 show the neutron fluence dependence of the spin densities in the high OH (T-1030) and low OH (T-2030) samples, respectively. Although the neutron fluence region is rather limited, it is observed that the spin densities of the E′s, NBOHCs, and PORs increase with the increasing neutron fluence while those of the X_1 and X_2 show some saturation behavior. This means that the X_1 and X_2 are of extrinsic and impurity-related centers. In fact, the spin densities of these states are higher and become saturated earlier in the high OH

Table 2
g-Values and peak-to-peak derivative widths determined in the present analysis[a]

Defects	g-Value			Peak-to-peak derivative width		
	g_1	g_2	g_3	σ_1	σ_2	σ_3
E′	2.0003	2.0005	2.0017	0.05	0.05	0.05
POR	2.002	2.007	2.067	0.1	0.2	1
NBOHC	2.001	2.010	2.08	0.1	0.3	3
X_1	1.996	2.015	2.17	0.2	0.4	4
X_2	1.992	2.021	2.22	0.3	0.5	4

[a] The λ and Δ values in Eqs. (1)–(3) were obtained to be $\lambda = 0.0527$ eV and $\Delta = 0.622$ eV for the X_1s and $\lambda = 0.0827$ eV and $\Delta = 0.752$ eV for the X_2s by employing $l = 1$ and $E = 5.08$ eV [4].

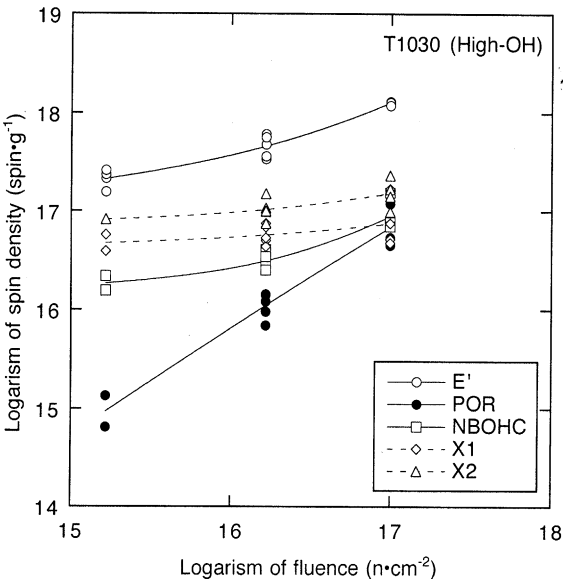

Fig. 2. Neutron fluence dependence of spin densities in the neutron-irradiated high OH silica (T-1030).

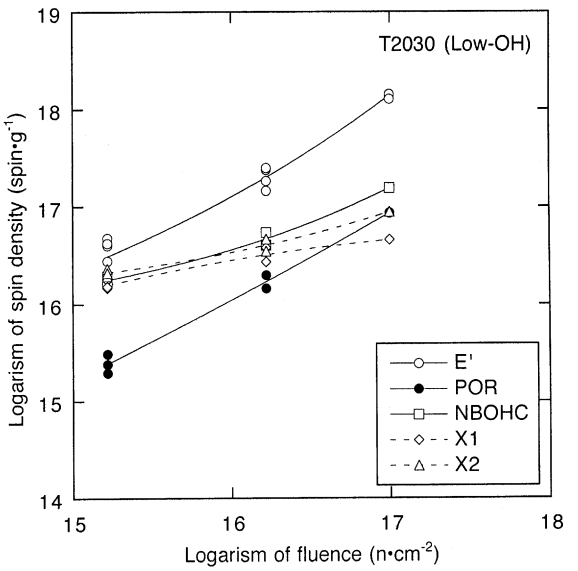

Fig. 3. Neutron fluence dependence of spin densities in the neutron-irradiated low OH silica (T-2030).

(T-1030) samples than in the low OH (T-2030) samples. Then it may be postulated that these states come from the impurity of OH. It is also noted that the spin densities of the E′ centers are higher in the high OH (T-1030) samples than in the low OH (T-2030) samples. Some additional production of the E′s is thus considered in the higher OH samples. No apparent difference due to different OH contents is observed for the PORs and NBOHCs.

The production of the E′s under irradiation may be expressed as

$$(\equiv Si{-}O{-}Si\equiv)^* \rightarrow \equiv Si^{\cdot} Si\equiv + O^- \tag{4}$$

where $(\equiv Si{-}O{-}Si\equiv)^*$ denotes an excited state produced by irradiation. Also, the PORs are produced from the E′s and O_2 molecules by [10]

$$\equiv Si^{\cdot} Si\equiv + O_2 \rightarrow \equiv Si{-}O{-}O^{\cdot} Si\equiv \tag{5}$$

Recently, Griscom and Mizuguchi [2] have pointed out that reaction (5) hardly occurs at lower temperatures since the activation energy ($E = 1.17$ eV [9]) for the O_2 diffusion is rather high. By considering this and by considering possible break up of the O_2 molecules by neutron irradiation [11], they have suggested the following reactions for the production of the NBOHCs and PORs at lower temperatures.

$$\equiv Si^{\cdot} Si\equiv + O^0 \rightarrow \equiv Si{-}O^{\cdot} Si\equiv \tag{6}$$

$$\equiv Si{-}O^{\cdot} Si\equiv + O^0 \rightarrow \equiv Si{-}O{-}O^{\cdot} Si\equiv \tag{7}$$

The O^0s are also produced by irradiation together with the diamagnetic ODCs [12] as

$$(\equiv Si{-}O{-}Si\equiv)^* \rightarrow \equiv Si : Si\equiv + O^0 \tag{8}$$

Thus the observed neutron fluence dependence of the spin densities of the E′s, NBOHCs, and PORs may be explained by considering these reactions, although it is needed to take into account the participation of the X_1s and X_2s in the reaction mechanisms.

For the presently observed X_1 and X_2 states, the following reactions can be suggested by considering that these states are produced together with the E′s from the impurity OH and by assuming that the O^-s are as mobile as the O^0s.

$$\equiv Si{-}OH + O^- \rightarrow \equiv Si^{\cdot} + O_2^- + H^0 \tag{9}$$

and/or

$$\equiv Si{-}OH + O^0 + e^- \rightarrow \equiv Si^{\cdot} + O_2^- + H^0 \tag{10}$$

The e^-s in reaction (10) may be supplied from such reactions under irradiation as

$$(\equiv Si{-}O{-}Si\equiv)^* \rightarrow \equiv Si{-}O^{\cdot} Si\equiv + e^- \tag{11}$$

$$(\equiv Si{-}O{-}Si\equiv)^* \rightarrow \equiv Si{-}\dot{O}{-}Si\equiv + e^- \tag{12}$$

Considering these reactions, it is explained that the spin densities of the E′s, X_1s and X_2s are sensitive to the OH content of the sample especially in the lower fluence region, increasing with the increasing OH content. When the spin density of the E′s increases, it is expected that reactions (6) and (7) occur and that the secondary production of the NBOHCs and PORs occur. However, such effects on the spin densities of the NBOHCs and PORs are hardly observed in the present case. This is possibly because the density of the O^0s is decreased by such reactions as reaction (10).

3.3. Isochronal anneal behavior of spin densities

Figs. 4 and 5 show the results of the isochronal anneal of high OH (T-1030) and low OH (T-2030) samples, respectively. The observed anneal behavior is well explained by considering the above reactions. For example, the spin densities of the E′s rapidly decrease below 473 K (200 °C) possibly due to their recombination with the mobile O^-s. Although the recombination is not completed below that temperature, the remaining E′s may recombine with the O_2^-s at higher temperatures at which the O_2^-s are expected to be as mobile as the O_2s.

Above 473 K (200 °C), the O_2s and O_2^-s become mobile, and their reactions start to occur. The spin densities of the X_1s and X_2s thus decrease with the increasing temperature in this range. The NBOHCs also decrease, for example, as

$$\equiv Si{-}O^{\cdot} Si\equiv + O_2^- \rightarrow \equiv Si{-}O{-}Si\equiv + O_2 \tag{13}$$

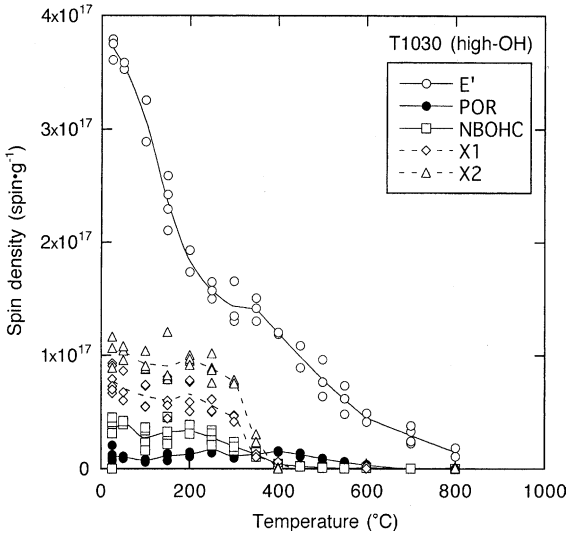

Fig. 4. Ten-minute isochronal anneal experiment of the neutron-irradiated high OH silica (T-1030). Neutron fluence: 1.6×10^{16} n cm^{-2}.

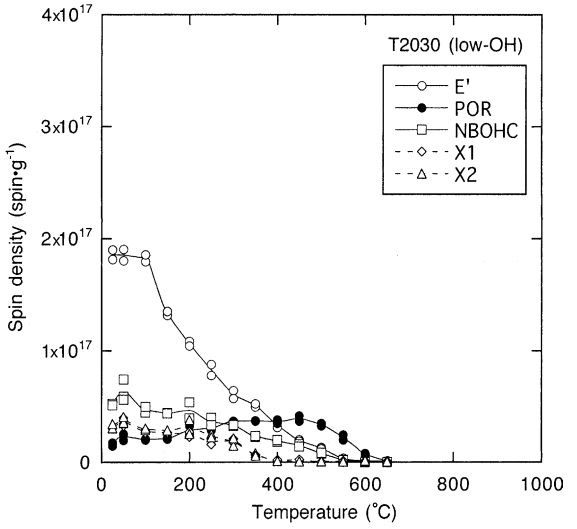

Fig. 5. Ten-minute isochronal anneal experiment of the neutron-irradiated low OH silica (T-2030). Neutron fluence: 1.6×10^{16} n cm^{-2}.

As shown in Figs. 4 and 5, the reactions of the PORs are somewhat different in different OH content samples. In the case of the low OH (T-2030) samples, the spin densities of the PORs increase with the increasing temperature up to 723 K (450 °C). This means reaction (5) occurs and a definite amount of the O_2s remains in this case. In the case of the high OH (T-1030) samples, on the other hand, reaction (5) hardly occurs. Because of reactions (9) and/or (10), not the O_2s but O_2^-s are considered to remain predominantly in this case.

4. Conclusions

In order to know the production behavior of irradiation defects in vitreous silica, the ESR measurements were performed in the present study. Some new states were observed in the ESR spectra together with the usual paramagnetic states of the E′ centers, non-bridging oxygen hole centers (NBOHCs), and peroxy radicals (PORs). The principal-axis g-values of the new states were obtained from the analysis, and were found to be typical of O_2^- ions in solids. Considering these defects, the observed effects of the OH content, neutron fluence, and post-irradiation isochronal anneal behaviors were well explained.

Since their production yield saturates with the increasing neutron fluence, the presently observed new states are of rather minor states and their production is hardly observed in the case of highly irradiated samples. However, it is important to take into account their participation in the reaction mechanisms.

Acknowledgements

The authors wish to thank Dr M. Okada and Dr T. Saito, Kyoto University, for their kind supports.

References

[1] L. Skuja, J. Non-Cryst. Solids 239 (1998) 16.
[2] D.L. Griscom, M. Mizuguchi, J. Non-Cryst. Solids 239 (1998) 66.
[3] W. Känzig, M.H. Cohen, Phys. Rev. Lett. 3 (1959) 509.
[4] J. Rolfe, J. Chem. Phys. 70 (1979) 2463.
[5] P.C. Taylor, P.J. Bray, J. Magn. Res. 2 (1970) 305.
[6] R.A.B. Devine, Phys. Rev. 35 (1987) 9783.
[7] D.L. Griscom, J. Non-Cryst. Solids 149 (1992) 137.
[8] T. Tabata, M. Hasegawa, M. Fujinami, Y. Ito, H. Sunaga, S. Okada, S. Yamaguchi, J. Nucl. Mater. 239 (1996) 228.
[9] F.J. Norton, Nature 191 (1961) 701.
[10] A.H. Edwards, W.B. Fowler, Phys. Rev. B 26 (1982) 6649.
[11] L. Skuja, B. Güttler, Phys. Rev. Lett. 77 (1997) 2093.
[12] K. Moritani, I. Takagi, H. Moriyama, J. Nucl. Mater. 312 (2003) 97.